

# Series Resistance Measurements of Perovskite Solar Cells Using $J_{sc}$ – $V_{oc}$ Measurements

Noemi Mundhaas, Zhengshan J. Yu, Kevin A. Bush, Hsin-Ping Wang, Jakob Häusele, Shaline Kavadiya, Michael D. McGehee, and Zachary C. Holman\*

The fill factor ( $FF$ ) of perovskite solar cells is considerably lower than that of gallium arsenide and silicon cells, though they have similar open-circuit voltage deficits. To probe the  $FF$  loss, which mainly comes from series resistance, the  $J_{sc}$ – $V_{oc}$  characterization technique is applied to perovskite solar cells. A continuous-lamp solar simulator with an array of neutral density filters is used instead of the quasi-steady-state photoconductance technique commonly employed for silicon cells, which allows us to tune sweep parameters to accommodate the complex behavior of perovskites such as hysteresis. It is found that, for  $\text{Cs}_{0.25}\text{FA}_{0.75}\text{Pb}(\text{Br}_{0.2}\text{I}_{0.8})_3$  (CsFA) perovskite cells, sweeping from positive to negative voltage yields the same series resistance regardless of sweep speed, whereas this is not the case if the sweep is reversed. However, for  $\text{CH}_3\text{NH}_3\text{PbI}_3$  perovskite cells, the series resistance is independent of the sweep speed in both sweep directions. It is also found that, for a poly[bis(4-phenyl)(2,4,6-trimethylphenyl)amine] (PTAA) hole contact, increasing the PTAA thickness barely changes the recombination-limited pseudo- $FF$ , but reduces the  $FF$  due to increased series resistance. A maximum  $FF$  of 80.9% was achieved with the PTAA hole contact on a CsFA perovskite absorber.

voltage deficits—defined as the difference between the bandgap voltage and open-circuit voltage ( $V_{oc}$ )—of only 0.37 V.<sup>[5]</sup> This is approaching the values of other mature solar technologies like gallium arsenide (GaAs). However, in contrast to the remarkable  $V_{oc}$ , the fill factor ( $FF$ ) of perovskite solar cells underperforms. As shown in **Figure 1**, which depicts the performance of champion devices with different absorbers, the  $FF$  of the best perovskite cell is only 79.6%. This is considerably lower than that of GaAs (86.5%) and monocrystalline silicon (84.9%), despite the wider bandgap and comparable  $V_{oc}$  deficit of the perovskite cells. To reach perovskite cell efficiencies in excess of 25%, understanding and overcoming  $FF$  losses is key.

The  $FF$  of a solar cell is governed, hierarchically, by recombination and series resistance ( $R_s$ ) at the maximum power point (MPP), in the absence of shunts. Assuming that the recombination at MPP is not wildly different from the recombination at open circuit, the small  $V_{oc}$  deficit in

The efficiency of perovskite solar cells has skyrocketed from 3.8 to 23.3% in the past few years and now rivals that of other technologies such as multi-crystalline silicon, cadmium telluride (CdTe), and copper indium gallium selenide (CIGS).<sup>[1,2]</sup> Thanks to long carrier lifetimes and thus high photoluminescence efficiencies,<sup>[3,4]</sup> the best perovskite cells now reach open-circuit


perovskite solar cells indicates that non-radiative recombination is not the primary reason for the  $FF$  loss. Few studies have linked materials in perovskite solar cells to their series resistance.<sup>[8–10]</sup> Kim et al. found that, for a 2,20,7,70-tetrakis(N,N-di-p-methoxyphenylamine)-9,9-spirofluorene (spiro-OMeTAD) hole contact, decreasing its thickness from 310 to 130 nm improved the  $FF$  of perovskite cells from 72.0 to 76.8% due to reduced series resistance.<sup>[8]</sup> Stolterfoht et al. found a similar dependence with a poly[bis(4-phenyl)(2,4,6-trimethylphenyl)amine] (PTAA) hole contact, consistent with their integrated time-of-flight measurements, which showed that the hole contact limits the carrier transport.<sup>[9]</sup> With an optimized hole contact, >80%  $FF$  was reported.<sup>[9]</sup> However, in these studies, the series resistance was calculated by fitting the one-sun current density–voltage ( $J$ – $V$ ) characteristic with a diode equation, which is prone to inaccuracies that can introduce errors as large as 6%, as demonstrated by Pysch et al.<sup>[11]</sup> and Kim et al.<sup>[8]</sup> In addition, the limiting  $FF$  of a perovskite cell that is free of series resistance—the so-called pseudo fill factor ( $pFF$ )—remains unclear. Although the above studies calculated  $pFF$  values of 85%<sup>[9]</sup> and 90%<sup>[10]</sup> for ideality factors of 1.5 and 1, respectively, they did so using an empirical expression from Green<sup>[12]</sup> that was derived

N. Mundhaas, Z. J. Yu, J. Häusele, S. Kavadiya, Z. C. Holman  
Arizona State University  
Tempe, Arizona 85281, USA  
E-mail: zachary.holman@asu.edu

N. Mundhaas, J. Häusele  
University of Konstanz  
Konstanz, Germany

K. A. Bush, H.-P. Wang, M. D. McGehee  
Stanford University  
Stanford, California 94305, USA

M. D. McGehee  
University of Colorado Boulder  
Boulder, Colorado 80309, USA

 The ORCID identification number(s) for the author(s) of this article can be found under <https://doi.org/10.1002/solr.201800378>.

DOI: 10.1002/solr.201800378

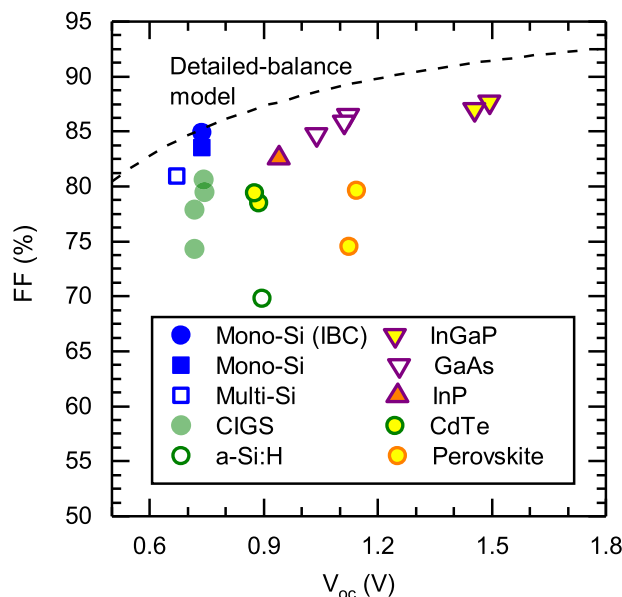


**Figure 1.** FF as a function of  $V_{oc}$  of record solar cells. The data were extracted from the *Solar Cell Efficiency Tables*.<sup>[1]</sup> Also shown are the (radiative-recombination-limited) FF limits, according to a detailed-balance model.<sup>[6,7]</sup>

for silicon solar cells operating in low injection. As we have previously demonstrated, this expression leads to absolute  $pFF$  errors of 6% for silicon cells under typical operating conditions and can lead to errors in excess of 10% in extreme cases.<sup>[13]</sup> Finally, these studies calculated series resistance for only a single sweep direction and sweep speed. Considering the hysteresis behavior of some perovskite cells, it is important to investigate the dependency of series resistance on these sweep parameters.

The series resistance at MPP is of most interest, as it characterizes the ideal operating condition of a solar cell.<sup>[11]</sup> In well-established silicon solar technology, a common way to measure series resistance starts with overlaying a one-sun  $J-V$  curve with a pseudo  $J-V$  curve, which is obtained from a Sinton Suns- $V_{oc}$  tool.<sup>[14]</sup> With this tool, the  $V_{oc}$  is probed as a function of illumination level during the decay of a light flash. This data is then used to construct a pseudo  $J-V$  curve that is free of series resistance, as no current flows during the measurement. Comparing the pseudo  $J-V$  curve with the one-sun  $J-V$  curve, one can determine series resistance at any illumination (and thus injection) level, including the MPP, by taking the voltage difference divided by the current density. This technique provides a more accurate determination of series resistance than fitting the one-sun  $J-V$  curve, and it yields  $pFF$  for any cell structure.<sup>[11]</sup>

The Sinton Suns- $V_{oc}$  setup has been previously used for other solar technologies such as kesterites and organic photovoltaics,<sup>[15,16]</sup> and would be extremely helpful for perovskite solar cells. However, the complex behavior of perovskite solar cells, especially the notorious hysteresis due to mobile ions,<sup>[17,18]</sup> limits its application because of the short flash decay time. Also, the built-in silicon reference cell in a Sinton tool introduces significant spectral mismatch when measuring other types of

solar cells, which requires non-trivial corrections for accurate measurements.<sup>[19]</sup>

Here, we apply the  $J_{sc}-V_{oc}$  technique, a predecessor of the Suns- $V_{oc}$  technique that was introduced by Wolf and Rauschenbach in 1963,<sup>[20]</sup> to perovskite solar cells with a continuous-lamp solar simulator equipped with neutral-density filters. With this setup, we measure one-sun and pseudo  $J-V$  curves of  $\text{Cs}_{0.25}\text{FA}_{0.75}\text{Pb}(\text{Br}_{0.2}\text{I}_{0.8})_3$  and  $\text{CH}_3\text{NH}_3\text{PbI}_3$  perovskite solar cells with the same (and tunable) measurement parameters, and without hysteresis.

Semitransparent and opaque  $\text{Cs}_{0.25}\text{FA}_{0.75}\text{Pb}(\text{Br}_{0.2}\text{I}_{0.8})_3$  (CsFA) perovskite solar cells, with the structures shown in Figure 2, were used in this study. To investigate the series resistance in perovskite solar cells, we first fabricated “baseline” semitransparent CsFA perovskite solar cells (Figure 2) and determined the voltage sweep speed that minimized hysteresis. Poly[bis(4-phenyl)(2,4,6-trimethylphenyl)amine] (PTAA) dissolved in chlorobenzene at  $5 \text{ mg mL}^{-1}$  concentration was spun on indium tin oxide (ITO) coated glass, purchased from Xinyan Technology, with a spin speed of 6000 rpm, followed by spin-coating of a 500-nm-thick CsFA perovskite layer. In one experiment, the CsFA perovskite was replaced with the common  $\text{CH}_3\text{NH}_3\text{PbI}_3$  (MAPI) perovskite for comparison. After that, a 40-nm-thick  $\text{C}_{60}$  layer was thermally evaporated on top of the perovskite layer, followed by 8-nm-thick tin oxide ( $\text{SnO}_2$ ) and 150-nm-thick ITO layers deposited by atomic layer deposition and sputtering, respectively. Finally, a silver grid was evaporated on top to complete the semitransparent cell. Details of the process were reported elsewhere.<sup>[21]</sup>

Next, we fabricated opaque CsFA perovskite solar cells in which the PTAA concentration was varied from 2.5 to 10  $\text{mg mL}^{-1}$ , with the same spinning settings, to investigate the role of the PTAA hole contact thickness in determining the series resistance of perovskite cells. The thickness of the PTAA layer was determined by matching the simulated external quantum efficiencies (EQE) of the solar cells in the 320–420 nm wavelength range—the PTAA absorption range—to their measured EQE. Optical simulations were performed using SunSolve, from PV Lighthouse,<sup>[22]</sup> using complex refractive indices reported elsewhere.<sup>[23]</sup> The resulting thicknesses ranged

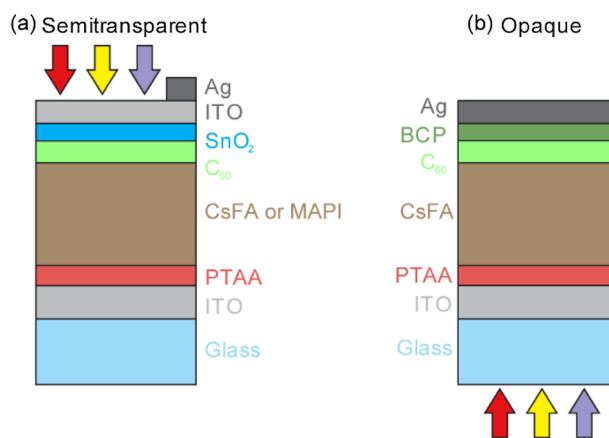


**Figure 2.** Schematics of the (a) semitransparent and (b) opaque perovskite solar cells investigated.

from 7 nm ( $2.5 \text{ mg mL}^{-1}$ ) to 23 nm ( $10 \text{ mg mL}^{-1}$ ). In contrast to the semitransparent cells, after spin-coating the perovskite layer and evaporating the  $\text{C}_{60}$  layer, the opaque cells were finished with 8-nm-thick bathocuproine (BCP) and 200-nm-thick Ag layers, both deposited by thermal evaporation. Details of the process were reported elsewhere.<sup>[24]</sup>

A Newport Oriel (92193A-1000) solar simulator and a Keithley 2440 source meter were used to measure  $J$ - $V$  curves, and neutral-density filters obtained from Sinton Instruments were used to vary the illumination intensity. At each reduced illumination level, the  $J_{sc}$  and  $V_{oc}$  were first recorded by sweeping a full  $J$ - $V$  curve between 1.2 V and  $-0.1$  V with 100 steps. These  $J_{sc}$ - $V_{oc}$  pairs were then converted into a pseudo  $J$ - $V$  curve using Equation (1), which reassigns a current value,  $J$ , to each measured  $J_{sc}^{\text{filtered}}$  value in accordance with the principle of superposition and the one-sun  $J_{sc}$  of the cell,  $J_{sc}^{1-\text{sun}}$ :

$$J(V_{oc}) = J_{sc}^{1-\text{sun}} \left[ \frac{1 - J_{sc}^{\text{filtered}}(V_{oc})}{J_{sc}^{1-\text{sun}}} \right] \quad (1)$$

Note that a constant cell temperature is a requirement for consistent  $V_{oc}$  measurements at different illumination levels, and thus we installed a cooling fan to minimize cell heating and frequently checked with a thermocouple that this was effective (maximum variation of  $3^\circ\text{C}$  across all measurements).

To validate our setup, we first measured  $J$ - $V$  curves of an amorphous silicon/crystalline silicon heterojunction cell under 14 filters and compared the results with those measured on a Sinton Suns- $V_{oc}$  tool. As shown in **Figure 3**, these 14  $J_{sc}$ - $V_{oc}$  points align with the results obtained from the Sinton tool. Fitting these points with a two-diode model yields  $pFF = 81.9\%$ , which is the same as that obtained from the Sinton tool.

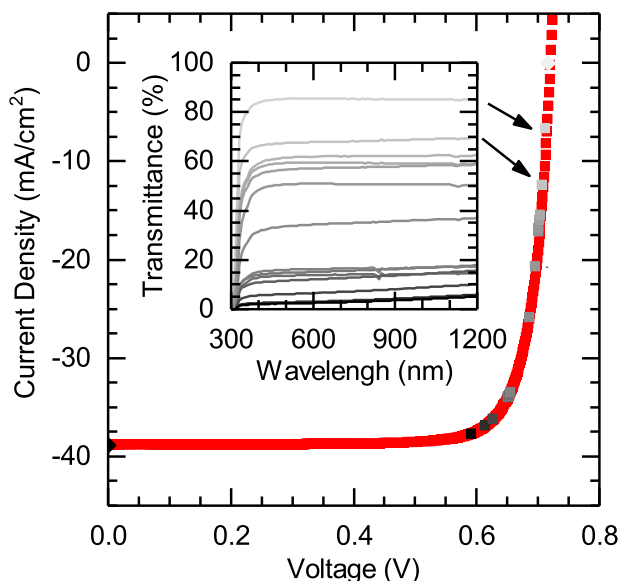


**Figure 3.** Pseudo  $J$ - $V$  curves of a silicon heterojunction cell measured with a Sinton Suns- $V_{oc}$  tool (red) and the  $J_{sc}$ - $V_{oc}$  setup (black). The inset shows the transmittance of the neutral-density filters.

**Figure 4a** shows one-sun  $J$ - $V$  and pseudo  $J$ - $V$  curves of a semitransparent CsFA perovskite solar cell under different sweep speeds and sweep directions. At fast sweep speeds (e.g.,  $0.55 \text{ V s}^{-1}$  and  $0.17 \text{ V s}^{-1}$ ), the one-sun  $J$ - $V$  curves show the signature of hysteresis. However, at slow speed ( $0.05 \text{ V s}^{-1}$ ), the hysteresis vanishes and the forward and reverse sweeps overlap. At each sweep speed, the pseudo  $J$ - $V$  curves are similar for both

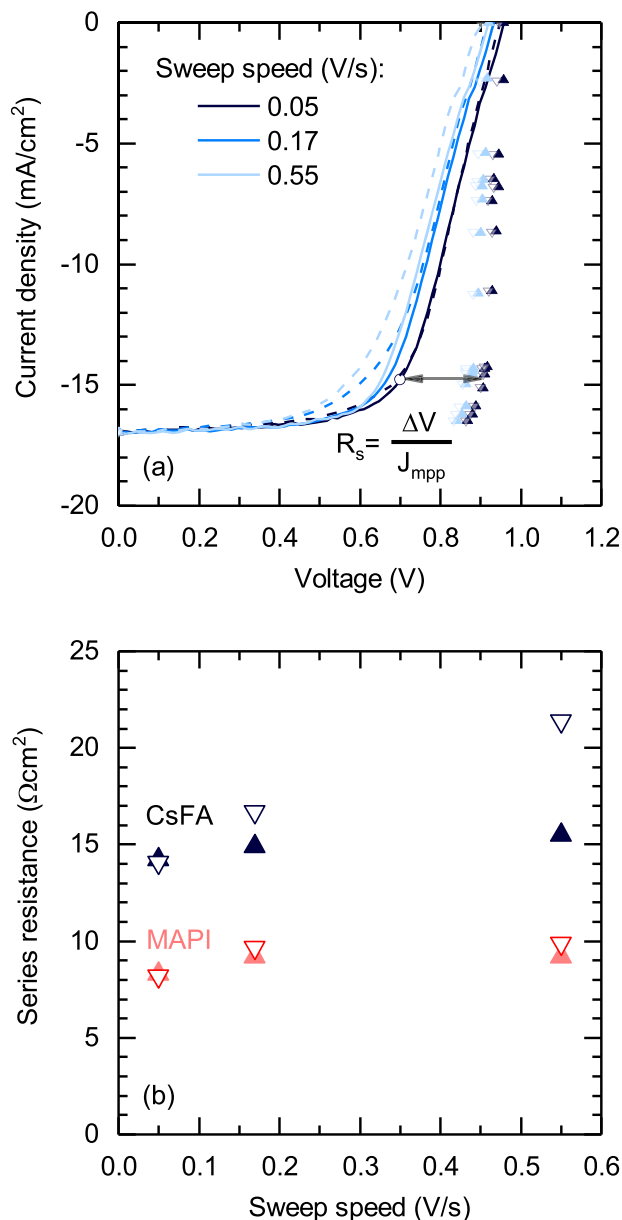


**Figure 4.** a) One-sun  $J$ - $V$  (lines) and pseudo  $J$ - $V$  (symbols) curves of a semitransparent CsFA perovskite solar cell measured with varying sweep speed. The arrow indicates the voltage difference between the pseudo and one-sun  $J$ - $V$  curves at MPP. b) Series resistance at MPP calculated from Figure 4a. Also shown is the series resistance of a MAPI cell with less hysteresis. The sweep direction from  $J_{sc}$  to  $V_{oc}$  is indicated with dashed lines ( $J$ - $V$  curves) and open symbols (pseudo  $J$ - $V$  curves and calculated resistances); the sweep direction from  $V_{oc}$  to  $J_{sc}$  is indicated with solid lines and solid symbols.

sweep directions. Figure 4b shows the series resistances at MPP calculated from Figure 4a. As expected, the resistances diverge at fast speed for different sweep direction and converge at slow speed. Interestingly, the series resistances are approximately the same when sweeping from  $V_{oc}$  to  $J_{sc}$ , regardless of sweep speed; even though the  $J$ - $V$  curves are shifted to lower voltages—likely due to unintentional preconditioning resulting from the varying sweep speed—the pseudo  $J$ - $V$  curves are also shifted to lower voltages, yielding a near-constant voltage difference at MPP. Figure 4b also shows the series resistance of a MAPI solar cell, characterized with the same methodology, that has less hysteresis and nearly the same series resistance for all sweep speeds and directions. We chose to sweep from  $V_{oc}$  to  $J_{sc}$  with the  $0.05 \text{ V s}^{-1}$  sweep speed for further experiments, as this seemed to yield the best balance between minimizing hysteresis and avoiding excessive cell heating.

Figure 5 shows the performance of opaque CsFA perovskite solar cells fabricated with different PTAA thicknesses. The perovskite cell with the thinnest PTAA layer of 7 nm achieved an efficiency of 16.9%, with a  $V_{oc}$  of 1.08 V,  $J_{sc}$  of  $19.3 \text{ mA cm}^{-2}$ , and a noteworthy  $FF$  of 80.9%. Within the PTAA thickness range investigated, the  $J_{sc}$  varies from  $19.0 \text{ mA cm}^{-2}$  to  $19.4 \text{ mA cm}^{-2}$ . The variation in current is caused by changes in the reflectance and parasitic absorptance, as confirmed by the EQE spectra (not shown), because these depend on the PTAA thickness when that layer is at the front of the cell. The  $V_{oc}$  varies by less than 40 mV and coincides with the  $J_{sc}$  trend. As the PTAA thickness increases, the efficiency drop is dictated by the  $FF$ . Figure 5c shows that the  $pFF$  of these cells, determined from  $J_{sc}$ - $V_{oc}$  measurements, stays almost constant, indicating that the surface recombination does not vary substantially with the PTAA thickness. The dramatic  $FF$  variation is thus dominated by series resistance. With PTAA thicknesses above 15 nm, the series resistance at MPP is higher than  $10 \Omega \text{ cm}^2$ , which results in  $FF$  below 70%. With a PTAA thickness of 5 nm, the champion device exhibits a  $pFF$  of 85.1% and a  $FF$  of 80.9%. The 4.2%

absolute  $FF$  loss that remains in this cell is caused by a series resistance of  $2.5 \Omega \text{ cm}^2$ , which could be from transport across the  $\text{C}_{60}$ /BCP electron contact or from other remaining resistance in the devices such as contact resistance, lateral transport resistance, or bulk resistance. Consistent with the findings of Stolterfoht et al.,<sup>[9]</sup> this comparatively low series resistance clearly shows that the PTAA hole contact limits carrier transport in this device. Further reducing the PTAA thickness may be expected to improve  $FF$ , but risks placing the lower-work-function ITO layer in direct contact with the perovskite absorber: cells made with  $1 \text{ mg mL}^{-1}$  PTAA concentration were all shunted.

The  $J_{sc}$ - $V_{oc}$  technique, implemented with a continuous-lamp solar simulator and neutral-density filters, can be used to quantify the resistive loss in perovskite solar cells at their operating point, thereby beginning the dissection of  $FF$ . As with one-sun  $J$ - $V$  measurements, care must be taken when measuring devices with hysteresis, as we observed that the series resistance can depend on the sweep speed and direction. Our measurements revealed that PTAA is an effective carrier-selective contact (capable of sustaining a high  $V_{oc}$ ) but is resistive even to the holes it collects. The series resistance that one can extrapolate as the PTAA thickness becomes vanishingly small sets an upper bound for the lumped resistance of the electron contact, and its comparatively small value of around  $2 \Omega \text{ cm}^2$  indicates that a  $\text{C}_{60}$ /BCP stack is much less resistive to electrons. This technique is a powerful tool for screening new electron and hole contacts for perovskite solar cells, and will be further strengthened by simple and robust methods to measure the individual components making up the series resistance.

## Acknowledgments

The information, data, or work presented herein was funded in part by the U.S. Department of Energy PVRD2 program under Award Number DE-EE0008167 and in part by the National Science Foundation under award No. 1664669.

## Keywords

fill factor,  $J_{sc}$ - $V_{oc}$ , perovskite, series resistance, suns- $V_{oc}$

Received: December 30, 2018

Revised: January 22, 2019

Published online:

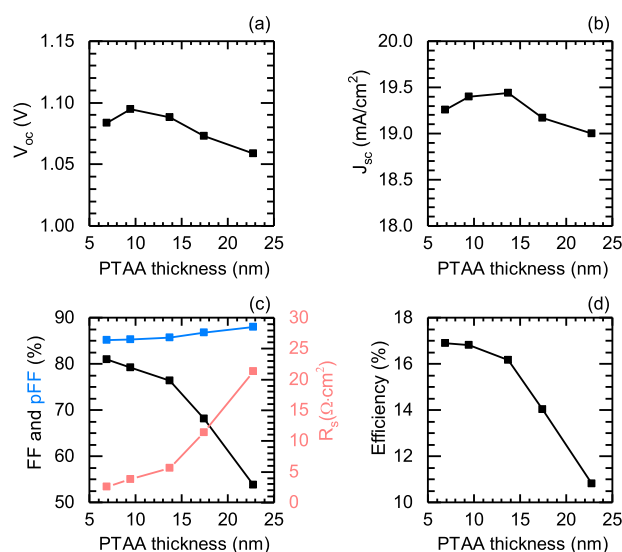


**Figure 5.** Performance of opaque CsFA perovskite cells with varied PTAA thickness. The calculated series resistances at MPP are shown in (c).

- [1] M. A. Green, Y. Hishikawa, E. D. Dunlop, D. H. Levi, J. Hohl-Ebinger, A. W. Y. Ho-Baillie, *Prog. Photovoltaics: Res. App.* **2018**, 26, 427.
- [2] NREL. Research Cell Record. Available: **2018**, <https://www.nrel.gov/pv/assets/pdfs/pv-efficiencies-07-17-2018.pdf>.
- [3] S. D. Stranks, G. E. Eperon, G. Grancini, C. Menelaou, M. J. P. Alcocer, T. Leijtens, L. M. Herz, A. Petrozza, H. J. Snaith, *Science* **2013**, 342, 341.
- [4] Q. Dong, Y. Fang, Y. Shao, P. Mulligan, J. Qiu, L. Cao, J. Huang, *Science* **2015**, 347, 967.
- [5] J. Huang, Y. Yuan, Y. Shao, Y. Yan, *Nat. Rev. Mater.* **2017**, 2, 17042.
- [6] Z. Yu, M. Leilaouioun, Z. Holman, *Nat. Energy* **2016**, 1, 16137.

- [7] W. Shockley, H. J. Queisser, *J. Appl. Phys.* **1961**, 32, 510.
- [8] H. D. Kim, H. Ohkita, *Solar RRL* **2017**, 1, 1700027.
- [9] M. Stollerfoht, C. M. Wolff, Y. Amir, A. Paulke, L. P. Toro, P. Caprioglio, et al. *Energy Environ. Sci.* **2017**, 10, 1530.
- [10] N. Wu, Y. Wu, D. Walter, H. Shen, T. Duong, D. Grant, C. Barugkin, X. Fu, J. Peng, T. White, K. Catchpole, K. Weber, *Energy Technol.* **2017**, 5, 1827.
- [11] D. Pysch, A. Mette, S. W. Glunz, *Sol. Energy Mater. Sol. Cells* **2007**, 91, 1698.
- [12] M. A. Green, *Solar Cells* **1982**, 7, 337.
- [13] M. Leilaouioun, Z. C. Holman, *J. Appl. Phys.* **2016**, 120, 123111.
- [14] R. Sinton, A. Cuevas, in *Proceedings of the 16th European Photovoltaic Solar Energy Conf.*, **2000**.
- [15] O. Gunawan, T. Gokmen, D. B. Mitzi, *J. Appl. Phys.* **2014**, 116, 084504.
- [16] S. Schiefer, B. Zimmermann, U. Würfel, *J. Appl. Phys.* **2014**, 115, 044506.
- [17] B. Chen, M. Yang, S. Priya, K. Zhu, *J. Phys. Chem. Lett.* **2016**, 7, 905.
- [18] E. L. Unger, E. T. Hoke, C. D. Bailie, W. H. Nguyen, A. R. Bowring, T. Heumüller, M. G. Christoforo, M. D. McGehee, *Energy Environ. Sci.* **2014**, 7, 3690.
- [19] T. Roth, J. Hohl-Ebinger, D. Grote, E. Schmich, W. Warta, S. W. Glunz, R. A. Sinton, *Rev. Sci. Instrum.* **2009**, 80, 033106.
- [20] M. Wolf, H. Rauschenbach, *Adv. Energy Conversion* **1963**, 3, 455.
- [21] K. A. Bush, A. F. Palmstrom, Z. J. Yu, M. Boccard, R. Cheacharoen, J. P. Mailoa, D. P. McMeekin, R. L. Z. Hoye, C. D. Bailie, T. Leijtens, I. M. Peters, M. C. Minichetti, N. Rolston, R. Prasanna, S. Sofia, D. Harwood, W. Ma, F. Moghadam, H. J. Snaith, T. Buonassisi, Z. C. Holman, S. F. Bent, M. D. McGehee, *Nat. Energy* **2017**, 2, 17009.
- [22] K. R. McIntosh, M. D. Abbott, B. A. Sudbury, S. Manzoor, Z. J. Yu, M. Leilaouioun, J. Shi, Z. C. Holman, in *2017 IEEE 44th Photovoltaic Specialist Conference (PVSC) Washington D. C.*, **2017**.
- [23] S. Manzoor, J. Häusele, K. A. Bush, A. F. Palmstrom, J. Carpenter, Z. J. Yu, S. F. Bent, M. D. McGehee, Z. C. Holman, *Opt. Express* **2018**, 26, 27441.
- [24] K. A. Bush, K. Frohna, R. Prasanna, R. E. Beal, T. Leijtens, S. A. Swifter, M. D. McGehee, *ACS Energy Lett.* **2018**, 3, 428.